Nonconservative higher-order hydrodynamic modulation instability

O. Kimmoun,[1,*] H. C. Hsu,[2] B. Kibler,[3] and A. Chabchoub[4,5,†]
[1]*Aix-Marseille University, CNRS, Centrale Marseille, IRPHE, Marseille, France*
[2]*Department of Marine Environment and Engineering, National Sun Yat-Sen University, Kaohsiung, Taiwan*
[3]*Laboratoire Interdisciplinaire Carnot de Bourgogne–UMR 6303 CNRS/Université Bourgogne Franche-Comté, 21078 Dijon, France*
[4]*Department of Mechanical Engineering, Aalto University, 02150 Espoo, Finland*
[5]*School of Civil Engineering, The University of Sydney, Sydney, NSW 2006, Australia*
(Received 14 March 2017; published 28 August 2017)

The modulation instability (MI) is a universal mechanism that is responsible for the disintegration of weakly nonlinear narrow-banded wave fields and the emergence of localized extreme events in dispersive media. The instability dynamics is naturally triggered, when unstable energy sidebands located around the main energy peak are excited and then follow an exponential growth law. As a consequence of four wave mixing effect, these primary sidebands generate an infinite number of additional sidebands, forming a triangular sideband cascade. After saturation, it is expected that the system experiences a return to initial conditions followed by a spectral recurrence dynamics. Much complex nonlinear wave field motion is expected, when the secondary or successive sideband pair that is created is also located in the finite instability gain range around the main carrier frequency peak. This latter process is referred to as higher-order MI. We report a numerical and experimental study that confirms observation of higher-order MI dynamics in water waves. Furthermore, we show that the presence of weak dissipation may counterintuitively enhance wave focusing in the second recurrent cycle of wave amplification. The interdisciplinary weakly nonlinear approach in addressing the evolution of unstable nonlinear waves dynamics may find significant resonance in other nonlinear dispersive media in physics, such as optics, solids, superfluids, and plasma.

DOI: 10.1103/PhysRevE.96.022219

I. INTRODUCTION

One possible explanation for the formation of extreme wave events, for instance, in the ocean and nonlinear optical media, is modulation instability (MI) [1–3]. Understanding the wave dynamics of modulationally unstable waves is of major significance for the sake of accurate modeling and prediction of localized structures as well as of rogue waves in particular [4,5]. The MI describes the disintegration of unidirectional and narrow-banded wave fields. Physically, the instability is driven, when sidebands that are located around the main carrier energy peak in a specific instability range are excited. The progressive focusing of the wave field is translated in the spectral domain with an advancing formation of an infinite number of sidebands in the form of a triangular cascade [6,7].

One deterministic way to study the MI is by use of the nonlinear Schrödinger equation (NLSE) [8,9]. This weakly nonlinear evolution equation is indeed very useful in the study of the problem, in view of its integrability [10]. In fact, the NLSE admits a family of exact solutions that model stationary, pulsating, and modulationally unstable wave fields [11]. The standard model that describes the MI process is the family of Akhmediev breathers (ABs) [12]. Indeed, for each unstable modulation frequency, or unstable sideband, one can assign an exact analytical AB expression to study the spatiotemporal evolution of the wave field. From an experimental perspective these universal types of solutions are very valuable, since the complex nonlinear physical processes can be controlled in time and space and adjusted to laboratory environments [13,14].

It is also known that for nonideal input conditions the wave field experiences a focusing recurrence after the first growth and decay cycle of instability, also known as Fermi-Pasta-Ulam (FPU) recurrence [6,15–17]. Interestingly, under particular conditions when the primary sidebands are shifted closer to the main frequency peak, the secondary or higher sidebands may also fall within the unstable frequency range. As a consequence, it is expected that focused wave packets undergo a pulse splitting followed by much complex nonlinear wave interaction compared to a *standard* FPU recurrence dynamics. This process is referred to as higher-order MI [18,19] and has been so far observed experimentally only in Kerr media [19,20].

In this paper, we report the observation of higher-order MI on the water surface using the framework of ABs, taking into account weak dissipation that is present in our laboratory setup and that impacts the nonlinear wave propagation motion. Experiments have been conducted in a unique and very large hydrodynamic wave facility, allowing the observation of a long-ranging evolution of unstable wave dynamics. We also show that weak dissipation, usually and naturally present in laboratory environments, may counterintuitively enhance the second recurrent focusing in a higher-order MI regime. The laboratory measurements, describing the higher-order dynamics, are in very good agreement with corresponding and nonconservative modified NLSE (MNLSE) simulations and justify the relevance of universal evolution equations in the study of nonlinear wave propagation in dispersive media.

*olivier.kimmoun@centrale-marseille.fr
†amin.chabchoub@aalto.fi

II. THEORETICAL FRAMEWORK

The dynamics of surface gravity waves in deep water can be described by the framework of the NLSE [21]

$$i\left(\Psi_x + \frac{2k}{\omega}\Psi_t\right) - \frac{k}{\omega^2}\Psi_{tt} - k^3|\Psi|^2\Psi = 0, \quad (1)$$

where g denotes the gravitational acceleration and k is the wave number of the narrow-banded as well as unidirectional wave field, that is connected to the wave frequency ω through the linear dispersion relation $k = \frac{\omega^2}{g}$. The NLSE is the simplest evolution equation that takes into account dispersion and nonlinearity of the wave dynamics. It can be also regarded as a universal evolution equation that describes wave dynamics in other fields of physics, such as solids [22,23], optics [4,24], superfluid helium [25], and plasma [26]. The particularity of the NLSE is its integrability. Indeed, it admits a number of stationary and pulsating localized envelope structures. One particular NLSE solution that describes the dynamics of MI of a Stokes wave of amplitude a is known as the Akhmediev breather [27]:

$$\Psi(X,T) = a\frac{\sqrt{2\mathfrak{a}}\cos(a\Omega T) + (1-4\mathfrak{a})\cosh(2a^2RX) + iR\sinh(2a^2RX)}{\sqrt{2\mathfrak{a}}\cos(a\Omega T) - \cosh(2a^2RX)}\exp(2a^2iX). \quad (2)$$

Here, $0 < \mathfrak{a} < 0.5$ denotes the breather parameter, $R = \sqrt{8\mathfrak{a}(1-2\mathfrak{a})}$ denotes the growth and decay rate, $\Omega = 2\sqrt{1-2\mathfrak{a}}$ denotes the modulation frequency, while $X = \frac{k^3}{2}x$ and $T = \sqrt{2}k^2(x - c_g t)$. Note that when $\mathfrak{a} \longrightarrow 0.5$ the modulation period becomes infinite, the growth becomes algebraic rather than exponential, and the wave dynamics is then described by the universal Peregrine breather solution [28–32]. The AB-type wave motion has been observed in a wide range of physical media and provides an ideal framework to control MI in space and time in laboratory environments [16,17,33]. In order to study numerically and/or experimentally the evolution dynamics of modulationally unstable Stokes waves, the initial input wave field of amplitude a can be determined by

$$\Psi(x = x_0, t) = a[1 + a_{\mathrm{mod}}\cos(\Omega t)]. \quad (3)$$

To ensure initial AB dynamics as described in Eq. (2), the relation between modulation amplitude a_{mod} and the modulation frequency Ω should be as follows: $\Omega = \sqrt{\frac{2R\mu i}{a_{\mathrm{mod}} - \mu}}$, where μ is a real parameter [16,34]. Even though experiments in optics and hydrodynamics can be well controlled, the presence of weak dissipation is inevitable. For water waves one possible source of dissipation is the viscosity. An effective model to take this into account is the addition of a linear attenuation factor of a wave envelope in the NLSE framework. Thus, for a given viscosity parameter ν the NLSE becomes [35,36]

$$i\left(\Psi_x + \frac{2k}{\omega}\Psi_t\right) - \frac{k}{\omega^2}\Psi_{tt} - k^3|\Psi|^2\Psi = -i\mathfrak{D}\Psi, \quad (4)$$

where $\mathfrak{D} = \frac{4k^3}{\omega}\nu$. It is also known that when ensuring a long propagation distance of the wave field the MI undergoes a recurrent focusing [6]. In this case, when only the primary sideband pair is within the unstable frequency range the unstable waves manifest FPU-like growth-decay cycles [16]. When weak dissipation is at play, the cycle exhibits a specific shift, commuting crest and trough dynamics in each focusing cycle [17]. In the presence of strong dissipation, the modulation instability can be also completely annihilated [37]. When the secondary or higher sideband pairs fall into the standard MI frequency range, a complex dynamics of the wave field arises from splitting of the focusing localized structures and in some cases is followed by a nonlinear interaction of wave envelopes [19].

Within the context of ABs, this can be achieved by shifting the modulation frequency towards $\Omega \longrightarrow 0$ or the breather parameter towards $\mathfrak{a} \longrightarrow 0.5$—more precisely, when $\mathfrak{a} \in]0.375; 0.5[$. We emphasize that higher-order MI dynamics can be also triggered from a three wave system with correct phase adjustment, choosing the sideband pair close to the carrier frequency accordingly, allowing the higher-order sidebands to lie in the unstable gain range [16,19]. The wave envelope splitting occurring after the first compression does not allow a return to the initial quasiregular condensate [19].

Figure 1 shows the dimensional wave dynamics of an AB model Eq. (2) for $\mathfrak{a} = 0.45$ as well as corresponding

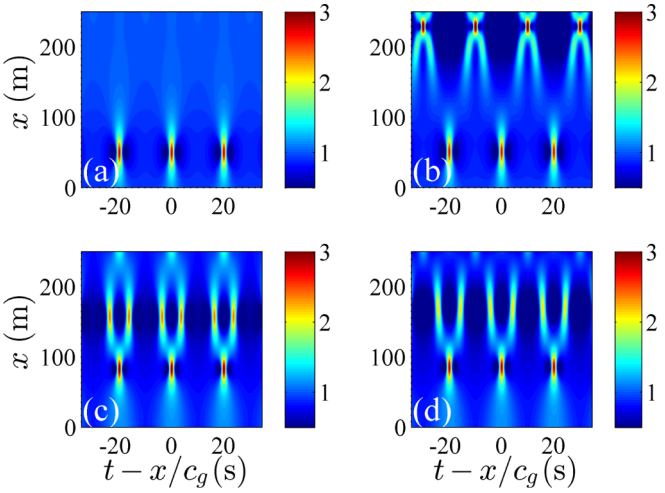

FIG. 1. Top left (a): NLSE envelope evolution simulations of a conservative AB. Top right (b): NLSE envelope evolution simulations of a dissipative AB with $\nu = 1.2\times10^{-5}$. Bottom left (c): NLSE simulations of a conservative envelope evolution with an approximated cosine modulation that fits the theoretical AB. Bottom right (d): NLSE simulations of a dissipative envelope evolution with an approximated cosine modulation that fits the theoretical AB with $\nu = 1.2\times10^{-5}$. The carrier parameters have been chosen to be $\varepsilon = ak = 0.12$ with amplitude $a = 0.03$ m at $x = -50$ m, the modulation frequency is determined by $\mathfrak{a} = 0.45$, while the envelope amplitudes have been normalized by the value of the amplitude a.

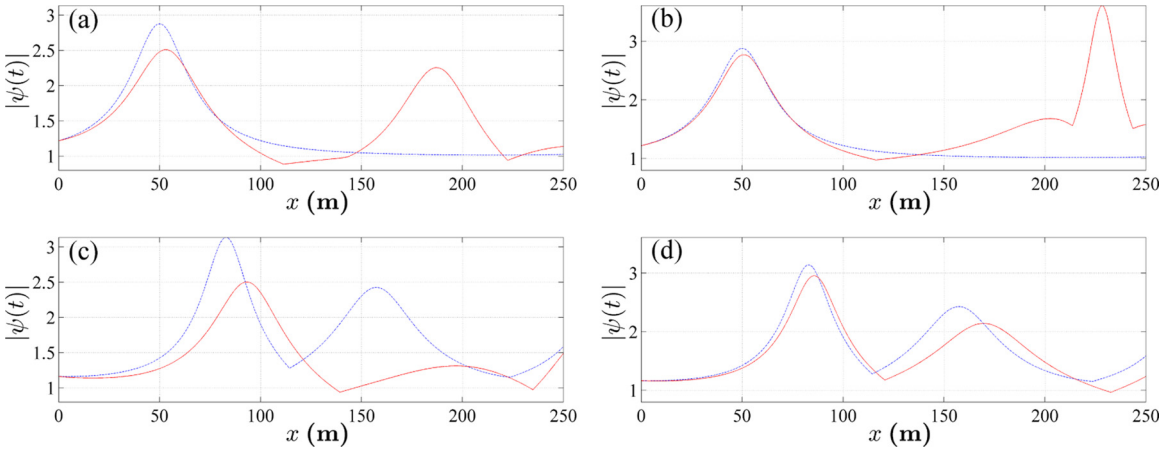

FIG. 2. Maximal wave amplitude amplifications $|\psi(t)|$ in the higher-order MI regime for carrier parameters $a = 0.03$ m and $\varepsilon = 0.12$ and $\mathfrak{a} = 0.45$ over a propagation distance of $x = 250$ m. Blue lines: Conservative dynamics. Red lines: Dissipative dynamics. Upper panels (a) and (b): AB dynamics. Lower panels (c) and (d): Corresponding cosine perturbation, as described by Eq. (3). Left panels (a) and (c): Dissipation rate is determined by $\nu = 1.2\times10^{-5}$. Right panels (b) and (d): Dissipation rate is determined by $\nu = 4.1\times10^{-5}$.

fitted periodic cosine envelope Eq. (3) in a conservative and dissipative context for carrier parameters $\varepsilon = ak = 0.12$ and $a = 0.03$ m. Clearly, a wave envelope pattern distinction can be noticed in the higher-order MI regime, either in the conservative or dissipative framework as well as either within the AB framework or cosine envelope approach approximation.

We would like to briefly point out that the dissipation parameter allows to control the complex spatiotemporal arrangement (nonlinear superposition) of breather-type structures. In fact, for each modulation frequency in this regime determined by $\mathfrak{a} \in]0.375; 0.5[$ we can find a set of dissipation parameters $\mathfrak{D}$, or alternatively ν, that engenders a collision of the *fissioned* ABs and as a result a significant focusing is expected due to the nonlinear interaction of these. Figure 2 shows the normalized maximal amplitude amplifications $\psi = \frac{\Psi}{a}$ reached in the case of the higher-order MI regime for an AB case and approximated cosine modulation in the conservative as well as dissipative framework. As expected, the first focusing is retarded when approximating the AB dynamics by a cosine modulation for $\mathfrak{a} = 0.45$, as described by Eq. (3) [16]. More interestingly, when dissipation is at play for the chosen dissipation value that is determined by $\nu = 1.2\times10^{-5}$ the following second wave focusing of the initial AB envelope is significantly more amplified. Indeed, this second focusing is shown to be much higher than expected from standard AB or standard MI predictions. Namely, it is beyond three times the amplitude of the background [21,38]. This type of dynamics at play for this case, as shown in the upper right and upper left panel of Figs. 1 and 2, respectively, resembles the formalism and observations of AB collisions [39] and confirms the possibility of wave focusing enhancement due to dissipation, as theoretically reported for the Benjamin Feir Index in [40], completing within the framework of breathers the complex picture of the nonlinear stage of modulation instability in a dissipative regime. The fact that these significant amplifications do not occur when approximating the AB envelope by a cosine approach shows the importance of phase-shift dynamics in the dissipative process.

III. EXPERIMENTAL RESULTS

Next, we describe the experimental as well as corresponding numerical investigation, related to higher-order MI wave dynamics on the water surface within the framework of AB envelope dynamics. Experiments have been conducted in a large water wave facility, installed at the Tainan Hydraulics laboratory. The facility has a length of 200 m with a constant water depth of 1.35 m while 60 capacitance wave gauges are installed along the flume. The small spacing between each wave probe allows a unique, precise, as well as accurate wave field acquisition. This is a decisive fact, when aiming for the reconstruction of the wave's envelopes in order to compare these with weakly nonlinear NLSE-type predictions. Figure 3 shows the schematic illustration of the water wave flume as well as the placement of the wave gauges along the facility.

In order to generate higher-order MI hydrodynamics we injected two different AB-type wave fields for $\mathfrak{a} = 0.45$, which

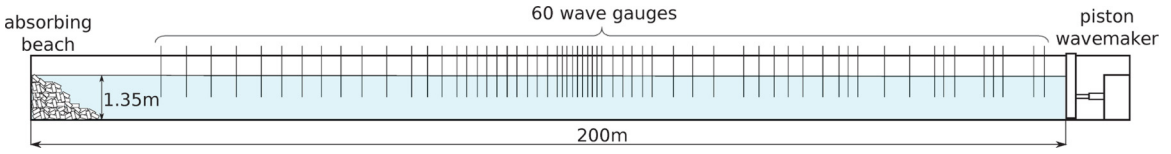

FIG. 3. Schematic description of the water wave facility, installed at the Tainan Hydraulics Laboratory.

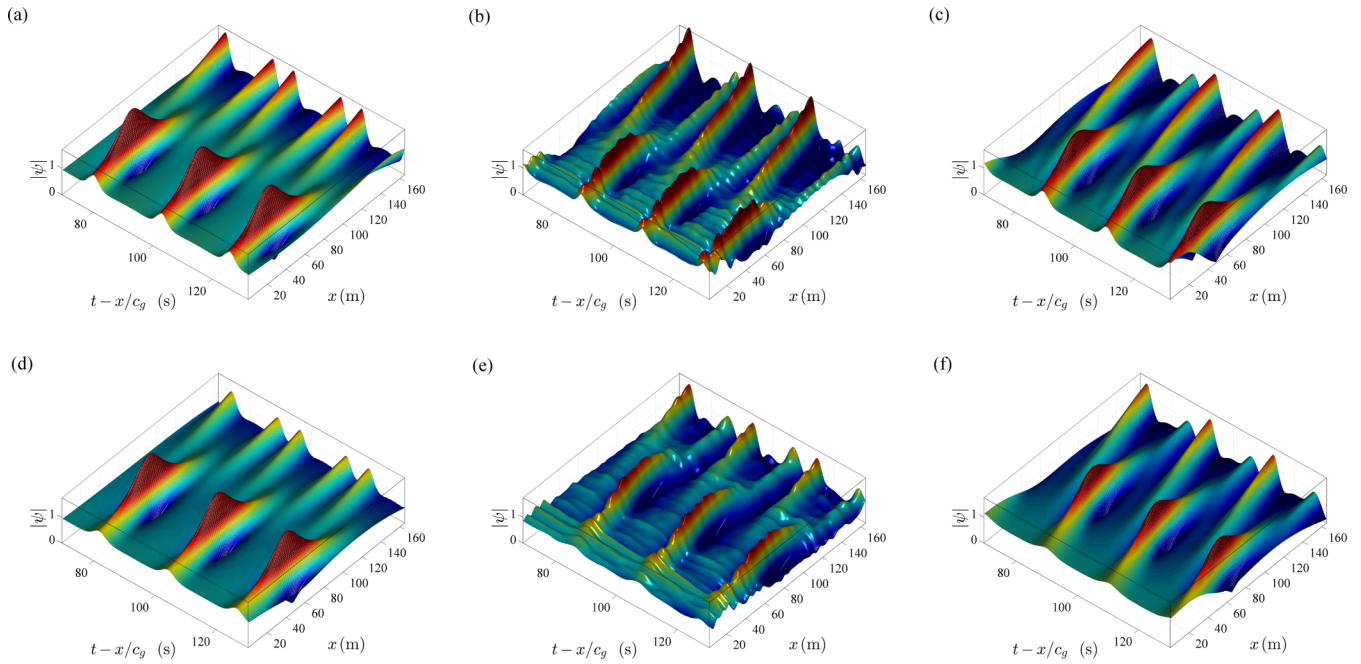

FIG. 4. From right to left: NLSE (4) simulations (a) and (d), experimental results (b) and (e), as well as MNLSE (5) simulations (c) and (f). Upper panels (a)–(c): AB wave envelope evolution with parameter $\mathfrak{a} = 0.45$ as well as carrier parameters $\varepsilon = 0.10$ and $a = 0.017$ m for $\nu = 2.2\times10^{-5}$. Bottom panels (d)–(f): AB evolution with parameter $\mathfrak{a} = 0.45$ as well as carrier parameters $\varepsilon = 0.12$ and $a = 0.03$ m for $\nu = 4.1\times10^{-5}$.

is the case when the second and third sideband pairs are within the unstable range with exponential growth rate [18,19,21]. The starting dynamics is initiated by taking into account small incipient envelope modulation, so that the first focusing occurs between 40 to 60 m from the wave maker. For the sake of validation of experimental results, the envelope of the measured water surface dynamics has been reconstructed, using the Hilbert transform [21] and then compared to NLSE and MNLSE simulations, including dissipation. The dissipative MNLSE formalism can be described by [36]

$$
\begin{aligned}
&i\left(\Psi_x + \frac{2k}{\omega}\Psi_t\right) - \frac{k}{\omega^2}\Psi_{tt} - k^3|\Psi|^2\Psi \\
&\quad = i\frac{k^3}{\omega}\{6|\Psi|^2\Psi_t + 2\Psi(|\Psi|^2)_t - 2i\Psi\mathcal{H}[(|\Psi|^2)_t]\} \\
&\qquad + i\frac{k^3}{\omega}\left(-4\nu\Psi - 20i\frac{\nu}{\omega}\Psi_t\right). \qquad (5)
\end{aligned}
$$

The linear dissipation rate $\mathfrak{D}$ has been determined in a prior experimental setting for a regular wave field with same corresponding wave parameters. Then, the parameter ν has been derived according to the relationship described in Eq. (4). The experimental results together with the numerical NLSE (4) and MNLSE (5) predictions are shown in Fig. 4.

Although the tank has a noticeable length of 200 m, we have not been able to observe the entire second focusing cycle that would reveal the corresponding complete dynamics of *fissioned* AB-type envelopes for the chosen wave and breather configuration parameters. However, we can clearly see the initialization of this focusing process, particularly, in the case shown in the upper panel of Fig. 4.

The propagation distance required to observe the latter nonlinear dynamics can be reduced by increasing the value of the wave steepness. However, increasing the steepness engenders breaking of these steep focused AB breather-type waves as a result of significant amplification, thus weakly nonlinear theories fail in describing such complicated wave dynamics [41]. Furthermore, due to the high wave amplitude amplifications reached for the chosen values of AB parameter $\mathfrak{a}$ as well as for the choice of carrier steepness, we can clearly notice and state that the MNLSE predictions are indeed more accurate than the NLSE model forecast. This can be notified in the asymmetry of wave envelope profiles in physical space. This is indeed well captured in the MNLSE approach and can be explained by assessing the effects of higher-order dispersion and mean flow [42–44]. The latter asymmetry is obviously also translated to an asymmetry in the spectral Fourier space. We also emphasize that the dissipation in the model, that is determined by the experiment in the specific laboratory environment, does not allow the observation of a second wave amplification focusing that is higher compared to the first focusing cycle. The corresponding spectral evolutions are depicted in Fig. 5. Note that we just turn our attention on the spectral dynamics around the carrier peak frequency and exclude the dynamics of the higher-order Stokes harmonics (bound waves), that is, frequencies around $\frac{\omega}{\pi}$, $\frac{3\omega}{2\pi}$, $\frac{2\omega}{\pi}$, etc., in the spectral domain. These spectral evolutions clearly show the nonlinear complexity of the wave dynamics at play as well as the expected presence of strong asymmetry around the main carrier energy. In addition, we can perceive the initialization of the second wave focusing, characterized by the beginning of spectral broadening that is clearly annotated. This is another clear proof for the quantitative accuracy of the MNLSE approach when studying higher-order MI

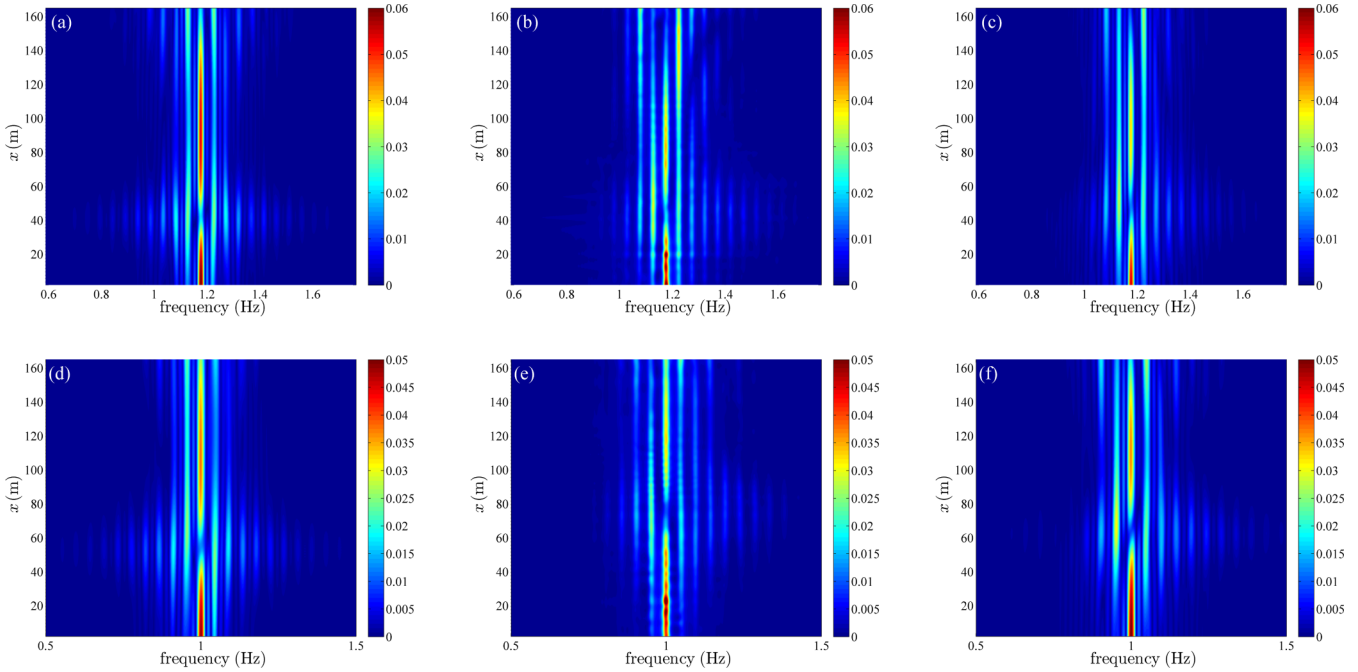

FIG. 5. From right to left: NLSE (4) (a) and (d), experimental (b) and (e), as well as MNLSE (5) spectral evolution of the wave field (c) and (f). Upper panels (a)–(c): Spectral dynamics along the wave flume with AB parameter $\mathfrak{a} = 0.45$ as well as carrier parameters $\varepsilon = 0.10$ and $a = 0.017$ m for $\nu = 2.2\times10^{-5}$. Bottom panels (d)–(f): Spectral dynamics along the wave flume with AB parameter $\mathfrak{a} = 0.45$ as well as carrier parameters $\varepsilon = 0.12$ and $a = 0.03$ m for $\nu = 4.1\times10^{-5}$.

processes. We annotate that the observed wave physics in the higher-order MI regime, as represented in the spectral domain, is utterly different than FPU dynamics. Indeed, after the spectral broadening, that is a result of wave focusing, the dynamical process does not return to a three wave system. This is also a first-time excellent comparison of long-term spectral evolution dynamics of MI in hydrodynamics.

IV. CONCLUSION

To conclude, we studied numerically and experimentally higher-order MI wave dynamics for surface gravity water waves in the presence of weak dissipation. The initial conditions for the experiments have been provided through the NLSE deterministic AB framework, complementing for instance experimental studies in optics in which the wave dynamics have been initiated from nonideal breather input conditions. We discussed the possibility of counterintuitive higher second wave focusing in a dissipative regime that is a result of AB-type envelope collision. The respective higher-order MI laboratory experiments reported are in very good agreement with numerical (dissipative) MNLSE simulations and confirm the applicability of weakly nonlinear models in the study of nonlinear water waves including extreme events, also when dissipation is at play. Furthermore, we showed that the dissipation parameter can be regarded as a new degree of freedom to control MI dynamics. We anticipate further studies in several nonlinear dispersive media with respect to higher-order MI, also to overcome the experimental limitations in hydrodynamics that are summarized in a short wave propagation distance and limited dissipation parameter range. Future work may be also devoted to the theoretical analysis of the effect of dissipation in the NLSE modeling [45,46] as well as prediction of extreme waves [47,48] in various physical media governed by the NLSE-type equations.

ACKNOWLEDGMENTS

O.K. acknowledges support from the French-Taiwanese ORCHID Program of the Hubert Curien Partnership (PHC). H.C.H. acknowledges grant support from the Taiwan Ministry of Science and Technology (MoST) Grants No. 104-2628-E-006-014-MY3, No. 105-2923-E-006-002-MY3, and No. 105-2611-I-006-301. B.K. acknowledges support from the French program Investissements d'Avenir, Project PIA2/ISITE-BFC. B.K. and A.C. are thankful for support from Burgundy Region (PARI Photcom).

[1] V. I. Bespalov and V. I. Talanov, Pis'ma Zh. Eksp. Teor. Fiz. **3**, 471 (1966) [Sov. Phys. JETP Lett. **3**, 307 (1966)].
[2] T. B. Benjamin and J. Feir, J. Fluid Mech. **27**, 417 (1967).
[3] G. Biondini and D. Mantzavinos, Phys. Rev. Lett. **116**, 043902 (2016).
[4] J. M. Dudley, F. Dias, M. Erkintalo, and G. Genty, Nat. Photon. **8**, 755 (2014).
[5] S. Residori, M. Onorato, U. Bortolozzo, and F. T. Arecchi, Contemp. Phys. **58**, 53 (2016).
[6] M. P. Tulin and T. Waseda, J. Fluid Mech. **378**, 197 (1999).

[7] V. E. Zakharov and L. A. Ostrovsky, Physica D **238**, 540 (2009).
[8] M. Lighthill, IMA J. Appl. Math. **1**, 269 (1965).
[9] V. E. Zakharov, J. Appl. Mech. Techn. Phys. **9**, 190 (1968).
[10] A. Shabat and V. Zakharov, Sov. Phys. JETP **34**, 62 (1972).
[11] N. Akhmediev and A. Ankiewicz, *Solitons: Nonlinear Pulses and Beams* (Chapman & Hall, London, 1997).
[12] N. Akhmediev, V. M. Eleonskii, and N. E. Kulagin, Sov. Phys. JETP **62**, 894 (1985).
[13] A. Chabchoub, M. Onorato, and N. Akhmediev, in *Rogue and Shock Waves*, edited by M. Onorato, S. Residori, and F. Baronio, Lecture Notes in Physics Vol. 926 (Springer, New York, 2016), p. 55.
[14] B. Kibler, J. Fatome, C. Finot, and G. Millot, in *Rogue and Shock Waves*, edited by M. Onorato, Lecture Notes in Physics Vol. 926 (Springer, New York, 2016), p. 89.
[15] E. Fermi, J. Pasta, and S. Ulam, Los Alamos Science Laboratory Report No. LA-1940, 1955 (unpublished); reprinted in *Collected Papers of Enrico Fermi*, edited by E. Segré (University of Chicago Press, Chicago, 1965), Vol. 2, p. 978.
[16] J. M. Dudley, G. Genty, F. Dias, B. Kibler, and N. Akhmediev, Opt. Express **17**, 21497 (2009).
[17] O. Kimmoun, H. Hsu, H. Branger, M. Li, Y. Chen, C. Kharif, M. Onorato, E. Kelleher, B. Kibler, N. Akhmediev, and A. Chabchoub, Sci. Rep. **6**, 28516 (2016).
[18] H. C. Yuen and B. M. Lake, Adv. Appl. Mech. **22**, 229 (1982).
[19] M. Erkintalo, K. Hammani, B. Kibler, C. Finot, N. Akhmediev, J. M. Dudley, and G. Genty, Phys. Rev. Lett. **107**, 253901 (2011).
[20] K. Hammani, B. Kibler, C. Finot, P. Morin, J. Fatome, J. M. Dudley, and G. Millot, Opt. Lett. **36**, 112 (2011).
[21] A. Osborne, *Nonlinear Ocean Waves and the Inverse Scattering Transform* (Academic Press, New York, 2010), Vol. 97.
[22] C. Chong, F. Li, J. Yang, M. O. Williams, I. G. Kevrekidis, P. G. Kevrekidis, and C. Daraio, Phys. Rev. E **89**, 032924 (2014).
[23] A. Grolet, N. Hoffmann, F. Thouverez, and C. Schwingshackl, Mech. Syst. Signal Proces. **81**, 75 (2016).
[24] P. Walczak, S. Randoux, and P. Suret, Phys. Rev. Lett. **114**, 143903 (2015).
[25] A. N. Ganshin, V. B. Efimov, G. V. Kolmakov, L. P. Mezhov-Deglin, and P. V. E. McClintock, Phys. Rev. Lett. **101**, 065303 (2008).
[26] H. Bailung, S. K. Sharma, and Y. Nakamura, Phys. Rev. Lett. **107**, 255005 (2011).
[27] N. N. Akhmediev, V. M. Eleonskii, and N. E. Kulagin, Theor. Math. Phys. **72**, 809 (1987).
[28] D. H. Peregrine, J. Aust. Math. Soc. Ser. B. Appl. Math. **25**, 16 (1983).
[29] B. Kibler, J. Fatome, C. Finot, G. Millot, F. Dias, G. Genty, N. Akhmediev, and J. M. Dudley, Nat. Phys. **6**, 790 (2010).
[30] A. Chabchoub, N. P. Hoffmann, and N. Akhmediev, Phys. Rev. Lett. **106**, 204502 (2011).
[31] L. Shemer and L. Alperovich, Phys. Fluids **25**, 051701 (2013).
[32] A. Tikan, C. Billet, G. El, A. Tovbis, M. Bertola, T. Sylvestre, F. Gustave, S. Randoux, G. Genty, P. Suret, and J. M. Dudley, Phys. Rev. Lett. **119**, 033901 (2017).
[33] A. Chabchoub, B. Kibler, J. Dudley, and N. Akhmediev, Phil. Trans. R. Soc. A **372**, 20140005 (2014).
[34] K. Hammani, B. Wetzel, B. Kibler, J. Fatome, C. Finot, G. Millot, N. Akhmediev, and J. M. Dudley, Opt. Lett. **36**, 2140 (2011).
[35] F. Dias, A. Dyachenko, and V. E. Zakharov, Phys. Lett. A **372**, 1297 (2008).
[36] J. D. Carter and A. Govan, Eur. J. Mech. B **59**, 177 (2016).
[37] H. Segur, D. Henderson, J. Carter, J. Hammack, C.-M. Li, D. Pheiff, and K. Socha, J. Fluid Mech. **539**, 229 (2005).
[38] M. Onorato, D. Proment, and A. Toffoli, Phys. Rev. Lett. **107**, 184502 (2011).
[39] B. Frisquet, B. Kibler, and G. Millot, Phys. Rev. X **3**, 041032 (2013).
[40] T. J. Bridges and F. Dias, Phys. Fluids **19**, 104104 (2007).
[41] A. Babanin, *Breaking and Dissipation of Ocean Surface Waves* (Cambridge University Press, Cambridge, England, 2011).
[42] K. B. Dysthe, Proc. R. Soc. A **369**, 105 (1979).
[43] K. Trulsen and C. T. Stansberg, in *Proceedings of the Eleventh International Offshore and Polar Engineering Conference*, 2001 (unpublished).
[44] E. Lo and C. C. Mei, J. Fluid Mech. **150**, 395 (1985).
[45] F. Baronio, M. Conforti, A. Degasperis, S. Lombardo, M. Onorato, and S. Wabnitz, Phys. Rev. Lett. **113**, 034101 (2014).
[46] B. Wetzel, D. Bongiovanni, M. Kues, Y. Hu, Z. Chen, S. Trillo, J. M. Dudley, S. Wabnitz, and R. Morandotti, Phys. Rev. Lett. **117**, 073902 (2016).
[47] W. Cousins and T. P. Sapsis, Phys. Rev. E **91**, 063204 (2015).
[48] S. Randoux, P. Suret, and G. El, Sci. Rep. **6**, 29238 (2016).